BNL-211939-2019-JAAM

No evidence for triose phosphate limitation of light saturated leaf photosynthesis under current atmospheric CO2 concentration

D. Kumarathunge, A. Rogers

To be published in "Plant, Cell and Environment"

July 2019

Environmental and Climate Sciences Department

Brookhaven National Laboratory

U.S. Department of Energy

USDOE Office of Science (SC), Basic Energy Sciences (BES) (SC-22)

Notice: This manuscript has been authored by employees of Brookhaven Science Associates, LLC under Contract No. DE-SC0012704 with the U.S. Department of Energy. The publisher by accepting the manuscript for publication acknowledges that the United States Government retains a non-exclusive, paid-up, irrevocable, world-wide license to publish or reproduce the published form of this manuscript, or allow others to do so, for United States Government purposes.

DISCLAIMER

This report was prepared as an account of work sponsored by an agency of the United States Government. Neither the United States Government nor any agency thereof, nor any of their employees, nor any of their contractors, subcontractors, or their employees, makes any warranty, express or implied, or assumes any legal liability or responsibility for the accuracy, completeness, or any third party's use or the results of such use of any information, apparatus, product, or process disclosed, or represents that its use would not infringe privately owned rights. Reference herein to any specific commercial product, process, or service by trade name, trademark, manufacturer, or otherwise, does not necessarily constitute or imply its endorsement, recommendation, or favoring by the United States Government or any agency thereof or its contractors or subcontractors. The views and opinions of authors expressed herein do not necessarily state or reflect those of the United States Government or any agency thereof.

Title: No evidence for triose phosphate limitation of light saturated leaf photosynthesis under current atmospheric CO_2 concentration

Authors: Dushan P. Kumarathunge[1,2*], Belinda E. Medlyn[1], John E. Drake[1,3], Alistair Rogers[4], Mark G. Tjoelker[1]

[1]Hawkesbury Institute for the Environment, Western Sydney University, Locked Bag 1797, Penrith, NSW 2751, Australia

[2]Plant Physiology Division, Coconut Research Institute of Sri Lanka, Lunuwila 61150, Sri Lanka

[3]Forest and Natural Resources Management, College of Environmental Science and Forestry, State University of New York, 1 Forestry Drive, Syracuse, NY 13210, USA

[4]Environmental and Climate Sciences Department, Brookhaven National Laboratory, Upton, NY 11973, USA

***Author for correspondence:** Dushan P. Kumarathunge

Email: dkumarathunge@gmail.com

Tel: +94 312255300

Key words: Terrestrial biosphere models, C_3 photosynthesis, AC_i curves, temperature, maximum carboxylation capacity, potential electron transport rate

Abstract

The triose phosphate utilization rate (*TPU*) has been identified as is one of the processes that can limit terrestrial plant photosynthesis. However, we lack a robust quantitative assessment of *TPU* limitation of photosynthesis at the global scale. As a result, *TPU*, and its potential limitation of photosynthesis, is poorly represented in terrestrial biosphere models (TBMs). In this study, we utilised a global dataset of photosynthetic CO_2 response curves representing 141 species from tropical rainforests to Arctic tundra. We quantified *TPU* by fitting the standard biochemical model of C_3 photosynthesis to measured photosynthetic CO_2 response curves, and characterised its instantaneous temperature response. Our results demonstrate that *TPU* does not limit leaf photosynthesis at the current ambient atmospheric CO_2 concentration. Furthermore, our results showed that the light saturated photosynthetic rates of plants growing in cold environments are not more often limited by *TPU* than those of plants growing in warmer environments. In addition, our study showed that the instantaneous temperature response of *TPU* is distinct from temperature response of the maximum rate of Rubisco carboxylation. The new formulations of the temperature response of *TPU* derived in this study may prove useful in quantifying the biochemical limits to terrestrial plant photosynthesis and improve the representation of plant photosynthesis in TBMs.

Introduction

Terrestrial biosphere models (TBMs) are one of the principal tools used to estimate the impact of climate change on terrestrial vegetation (Medlyn et al., 2011; Mercado et al., 2018; Rogers et al., 2017). Plant photosynthesis is one of the key components in these models. Robust representation of photosynthesis and its response to climate change are important for predicting the response of terrestrial vegetation to global change. Many TBMs incorporate the Farquhar et al., (1980) biochemical model of C_3 photosynthesis (FvCB hereafter) to estimate terrestrial gross primary productivity (GPP) (Rogers et al., 2017). Hence, the effect of climate change on modelled GPP depends on the formulation and parameterisation of the FvCB model, and in particular, on the sensitivity of the key model parameters to environmental variables such as temperature, atmospheric CO_2 concentration and soil moisture (Smith & Dukes 2013).

The FvCB model mechanistically represents photosynthetic CO_2 assimilation as the minimum of two biochemical processes: Rubisco carboxylation, and ribulose-1,5-bisphosphate (RuBP) regeneration (von Caemmerer, 2013; Farquhar et al., 1980). However, under some environmental conditions, a third biochemical process, the triose phosphate utilization rate (*TPU*), limits net photosynthesis (Harley & Sharkey; 1991; McClain & Sharkey, 2019; Sharkey, 1985; Sharkey et al., 2007). Decades of empirical research has sought to improve the model representation of the first two processes (Hikosaka et al., 2006; Kattge & Knorr, 2007; Kumarathunge et al., 2018a, Medlyn et al., 2002; Rogers et al., 2017; Wullschleger, 1993). In contrast, *TPU* is often ignored when parameterising the FvCB model (Crous et al., 2013; De Kauwe et al., 2016; Manter & Kerrigan, 2004; Vårhammar et al., 2015) and is rarely implemented in TBMs (Kattge, Knorr, Raddatz, & Wirth, 2009; Smith et al., 2017; Smith et al., 2016). Although we have a sound biochemical understanding of the *TPU* limitation on plant photosynthesis (Sharkey, 1985), we lack a robust quantitative

assessment of *TPU* limitation of photosynthesis at the global scale. There is a dearth of empirical evidence of environmental controls on *TPU* limitation across different plant functional types and biomes (Lombardozzi *et al.* 2018) which is a critical knowledge gap limiting informed implementation of TBM formulations that include *TPU* limitation as part of the FvCB model (Rogers *et al.* 2017).

Empirical studies demonstrate that *TPU* limitation occurs more frequently at higher CO_2 concentration (Busch & Sage, 2017; Labate & Leegood, 1988; Sage et al., 1989), but it is not clear to what extent it limits photosynthesis at current or future predicted atmospheric CO_2 concentrations. Some studies indicate that net photosynthesis is more likely to be *TPU* limited at low temperatures even under ambient CO_2 concentrations (Busch & Sage, 2017; Sage & Sharkey, 1987; Stitt & Hurry, 2002; Strand et al., 1997; Yang et al., 2016), but it is not clear how widespread this finding might be. At low temperatures, due to lower activity of proteins of the sucrose synthesis pathway (e.g. cytosolic fructose-1,6-bisphosphatase, sucrose phosphate synthase), the rate of triose phosphate production in the Calvin cycle cannot be met by the capacity of sucrose synthesis (Pons, 2012). Due to this over-proportional decrease in sucrose synthesis, it can be expected that *TPU* limitation would be more frequent at low temperatures (Sharkey *et al.*, 1986, Stitt *et al.*, 1988). Hence, it can be hypothesised that TPU limitation of photosynthesis is more prevalent in plants growing at cold environments compared to the plants grown at warm environments. Nevertheless, several lines of evidence suggested that sucrose synthesis capacity is increased as the plants acclimate to low temperatures (Stitt & Hurry, 2002). Also, previous literature suggested that plants regulate *TPU*, Rubisco activity, and RuBP regeneration so that the capacity to fix carbon will not exceed the capacity to make sugars (Stitt & Grosse, 1988, Stitt *et al.*, 1988). Further, plants maintain *TPU* rate just slightly higher than what is likely to be required (Yang et al., 2016). Hence, it is also likely that photosynthesis of cold acclimated plants is less likely to be

limited by *TPU* as has been observed previously in a limited number of species (Sage & Sharkey, 1987). However, it is not clear to what extent that *TPU* limits photosynthesis in plants growing in the diverse range of different growth temperatures that are represented by TBMs. Most studies on *TPU* limitation have been conducted under controlled experimental conditions (Bernacchi *et al.* 2013). Evidence for the occurrence of *TPU* limitation in mature plants in natural ecosystems is rare (Ellsworth, Crous, Lambers, & Cooke, 2015). Owing to this lack of evidence, many TBMs either do not consider *TPU* limitation or represent it non-mechanistically (Rogers *et al.* 2017, Lombardozzi *et al.* 2018). For example, some models assume *TPU* to be a fixed fraction of the maximum rate of Rubisco carboxylation (V_{cmax}), where W_p=0.5V_{cmax} (Clark et al., 2011,Oleson et al 2013; Collatz et al., 1991). Moreover, these models assume that the temperature response of *TPU* is identical to that for V_{cmax} (e.g. Oleson et al., 2013). Studies of the temperature response of *TPU* are also rare (Yang et al., 2016), so there are limited resources available to inform the adoption of an independent *TPU* temperature response in TBMs.

Recently, Lombardozzi *et al* (2018) examined the effect of including *TPU* limitation in the Community Land Model v4.5 (CLM). They found that implementation of *TPU* in CLM resulted in a limitation of photosynthesis by *TPU* under present day and future predicted ambient CO_2 concentrations, most consistently at high latitudes, and an approximate 6% reduction in terrestrial carbon uptake and storage at the end of the 21st century. To represent *TPU*, the following assumptions were made. Firstly, *TPU* was assumed to be a fixed fraction of V_{cmax}. Secondly, the temperature response of *TPU* was assumed to be the same as for V_{cmax}. Thermal acclimation of *TPU* was assumed to be the same as that of V_{cmax}, which was represented by an algorithm derived from empirical data (Kattge & Knorr 2007). Owing to the limitations of that empirical dataset, the algorithm does not allow for temperature acclimation below 11°C or above 29°C. Lombardozzi et al., (2018) highlighted the need for

improved physiological understanding of the conditions under which *TPU* limitation might be important, and the need for empirically-informed implementation of *TPU* in TBMs. However, to date, there is no comprehensive study available in the literature that can enable an assessment of *TPU* in response to the environment. Therefore, the validity of the above assumptions, and similar ones in other TBMs (Rogers et al., 2017; Smith & Dukes, 2013) remains uncertain. Given the sensitivity of terrestrial plant photosynthesis to *TPU* in current TBMs, as highlighted by Lombardozzi et al., (2018), it is important to synthesise the extent of *TPU* limitation and its temperature response using data obtained across different ecosystems at the global scale.

To address this knowledge gap, we used a global dataset of plant photosynthetic CO_2 response curves spanning ecosystems from tropical rainforests to Arctic tundra. We inferred key photosynthetic biochemical parameters by fitting a standard C_3 photosynthesis model to the raw gas exchange data. Our primary objective was to improve the current understanding of *TPU* limitation on leaf net photosynthesis by describing and summarising the extent of *TPU* limitation across important plant functional types grown and measured in their natural environments around the globe. In particular, we examined the following three questions: (1) Is *TPU* limitation to leaf photosynthesis widespread at current ambient atmospheric CO_2 concentrations? (2) Is the photosynthetic rate of plants growing in cold environments more often limited by *TPU* than in plants growing in warmer environments? (3) Do *TPU* and V_{cmax} have similar instantaneous temperature responses?

Materials and methods

Data sources

We used AC_i-TGlob_V1.0 (Kumarathunge et al., 2018b), a global dataset of plant photosynthetic CO_2 response curves (referred to as A/C_i curves hereafter) for this analysis. The dataset contains a total of 5113 A/C_i curves measured *in situ* at multiple leaf temperatures of upper canopy sun-lit leaves from 141 plant species from 42 different studies conducted around the world (Table S1). The dataset covers diverse ecosystems including tropical rainforests, temperate and boreal forests, semi-arid woodlands and Arctic tundra. A detailed description of data collection, data compilation and quality control is given in Kumarathunge et al., (2018b).

Theory

We used the Farquhar et al. (1980) C_3 photosynthesis model to infer the biochemical limitations on net leaf photosynthesis (A_{net}). The model incorporates three principal processes occurring in plant leaves at the same time: photosynthesis, photorespiration and mitochondrial respiration in the light (Farquhar et al. 1980). The original FvCB model represents A_{net} as the minimum of two process rates: the Rubisco carboxylation limited photosynthetic rate (W_c), the RuBP-regeneration limited photosynthetic rate (W_j), and later revised to include the triose phosphate utilization limited rate, W_p (Sharkey 1985; Harley & Sharkey 1991). The widely used formulation of the model is as follows:

$$A_{net} = \min\left(W_c, W_j, W_p\right)\left(1 - \frac{\Gamma^*}{C_i}\right) - R_L \qquad \text{Eqn 1}$$

$$W_c = V_{cmax}\frac{C_i}{C_i + K_c\left(1 + \frac{O_i}{K_o}\right)} \qquad \text{Eqn 2}$$

$$W_j = \frac{J}{4}\frac{C_i}{(C_i + 2\Gamma^*)} \qquad \text{Eqn 3}$$

$$W_p = \frac{3TPU\ C_i}{C_i - (1+3\alpha)\Gamma^*} \qquad \text{Eqn 4}$$

where V_{cmax} is the maximum rate of carboxylation by the enzyme ribulose-1,5-bisphosphate carboxylase-oxygenase (Rubisco), C_i and O_i (µmol mol^{-1}) are intercellular CO_2 and O_2 concentrations respectively, K_c and K_o (µmol mol^{-1}) are Michaelis–Menten coefficients of Rubisco activity for CO_2 and O_2 respectively, Γ^* (µmol mol^{-1}) is the CO_2 compensation point in the absence of photorespiration, R_L (µmol m^{-2} s^{-1}) is the non-photorespiratory CO_2 evolution in the light, J (µmol m^{-2} s^{-1}) is the rate of electron transport which is related to incident photosynthetically active photon flux density (Q, µmol m-2 s-1) by Eqn 5 , *TPU* (µmol m^{-2} s^{-1}) is the triose phosphate utilization rate, and α is the fraction of the photorespiratory product, glycolate, returned to the chloroplast. We assumed α =0 (a closed photorespiratory cycle; Harley & Sharkey 1991) when fitting A/Ci curves.

$$\theta J^2 - (\phi Q + J_{max})J + \phi Q J_{max} = 0 \qquad \text{Eqn 5}$$

where *Jmax* (µmol m^{-2} s^{-1}) is the potential rate of electron transport, ϕ (µmol mol^{-1}) is the quantum yield of electron transport, and θ (dimensionless) is the curvature of the light response curve

We fitted Eqns 1 – 5 to each measured A/C_i curve using the *fitacis* function within the plantecophys package (Duursma, 2015) in R version 3.5.1 (R Development Core Team, 2018). The model fitting algorithm is based on the logic introduced by (Gu et al., 2010). Fitting is done by looping over the potential limitation states. The different limitation states are obtained by assigning each point in an A/C_i curve to one of three limitations, without a prior assumption in the order of each limitation states occur. Parameter values are obtained for each limitation state by regression. Parameter values are retained for the limitation state yielding the best overall fit with minimum sum of squares error (Duursma, 2015). This fitting approach is appropriate because it makes no *a priori* assumptions about the limitation states

at different parts of the curve. Some curves may show no *TPU*-limitation. We used the Bernacchi et al., (2001) kinetic constants for the temperature response of K_c, K_o and Γ^* as given in Medlyn et al., (2002). We used measured photosynthetically active irradiance values (PAR) for fitting A/C_i curves whenever available, otherwise assuming a fixed value of 1800 μmol m^{-2} s^{-1}. We assumed default *fitacis* parameter values for quantum yield of electron transport; Φ (0.24 mol mol^{-1}) and the curvature of the light response curve, θ (0.85; unitless) for all datasets (Eqn 5). In our A/C_i curve fitting method, we did not account for the variations in mesophyll conductance (g_m) as g_m is not separately identifiable from V_{cmax} when fitting an A/C_i curve. Therefore, the estimated parameters, V_{cmax} and J_{max}, are considered apparent values (Bahar et al., 2018). This approach is appropriate for this analysis because almost all current TBMs ignore g_m and use apparent V_{cmax} and J_{max} values. We did not account for CO_2 and H_2O diffusion through cuvette gaskets as there was insufficient information to implement those corrections accurately across the large set of curves. We visually inspected every fitted A/Ci curve in the dataset for possible outliers and erroneous data points (i.e. negative intercellular CO_2 concentrations). We excluded parameters of a given A/C_i curve from further analysis if the r^2 of the fitted function was less than 0.90 (De Kauwe et al., 2016). This criterion removed approximately 6% of the total A/C_i curves of the dataset. After screening, the dataset contained a total of 4260 A/C_i curves measured at leaf temperatures ranging from 3 to 50°C. A detailed description of the A/C_i curve fitting and parameter quality control can be found in Kumarathunge et al. (2018a).

We utilised the intercellular CO_2 concentration at the rate transition points to infer the biochemical process that limits the net photosynthetic rate at current ambient CO_2 levels (400 μmol mol^{-1}). The C_i transition points between W_c and W_j ($C_{i\text{-}1}$) and W_j and W_p ($C_{i\text{-}2}$) were located by identifying the points at which the two functions (i.e. either W_c and W_j or W_j and W_p) intersect (see Figure 1). We calculated the C_i corresponding to the current ambient CO_2

concentration of 400 µmol mol^{-1} by assuming a constant C_i:C_a of 0.7 (median C_i:C_a across the dataset; Figure S1), giving C_i=280 µmol mol^{-1}. Under these assumptions, we inferred that the photosynthetic rate at the current ambient CO_2 concentration is W_c limited if 280 ≤ C_{i-1} and C_{i-2}, W_j limited if C_{i-1} < 280 ≤ C_{i-2}, and W_p limited if C_{i-1} and C_{i-2} ≤ 280. A conceptual depiction of these conditions is shown in Figure 1.

Data analysis

The dataset utilised in this study contains data measured across a range of experiments including mature plants growing in their native environments, common garden studies and datasets with repeated seasonal photosynthetic measurements. Our objective was to summarize the extent of *TPU* limitation on leaf photosynthesis across the globe. First, we utilised all available data to quantify how frequently *TPU* is limiting at the current ambient CO_2 concentration. Secondly, we utilised a subset of the dataset which contains measurements from mature plants growing and measured in their native environments to identify patterns in *TPU* limitation across different ecosystems. To examine temperature responses of *TPU*, we further subset the data to only consider curves where *TPU* limitation was identified by the fitting algorithm. The temperature response of *TPU* was fitted using the peaked Arrhenius function (Johnson et al., 1942):

$$TPU_{(T_k)} = TPU_{25} exp\left[\frac{E_a(T_k - 298.15)}{(298.15\, R\, T_k)}\right] \frac{1 + exp\left(\frac{298.15\, \Delta S - H_d}{298.15\, R}\right)}{1 + exp\left(\frac{T_k\, \Delta S - H_d}{T_k\, R}\right)} \qquad \text{Eqn 6}$$

where $TPU_{(Tk)}$ is the process rate at a given temperature, T_k (K), TPU_{25} is the triose phosphate utilization rate at 25 ºC, R is the universal gas constant (8.314 J mol^{-1} K^{-1}), E_a (kJ mol^{-1}) is the activation energy term that describes the exponential increase in the temperature response function with the increase in temperature, H_d (kJ mol^{-1}) is the deactivation energy and ΔS (J mol^{-1} K^{-1}) is the entropy term. To avoid over-parameterization, we assumed a fixed value of

200 kJ mol^{-1} for H_d in Eqn 6 for all datasets (Dreyer et al., 2002). Parameters of Eqn 6 were estimated in a non-linear mixed model framework (Zuur et al., 2009) using the *nlme* function within the *nlme* package in R version 3.5.1 (R Development Core Team, 2018). We extracted the long-term (1960-1990) mean air temperature at the measurement sites using a high resolution global gridded climatology database (Hijmans, Cameron, Parra, Jones, & Jarvis, 2005). We calculated mean growing season temperature for each site as the mean temperature of the months with mean temperatures above 0 °C (T_{home}). We fitted general additive models (GAM) (Rigby and Stasinopoulos, 2005) to visualize the patterns in the basal rate of *TPU* (TPU_{25}) of mature plants with mean growing season temperature of the native growth environment (Q2). The R code used for the entire analysis is publicly available through the repository, https://bitbucket.org/Kumarathunge/testtpu.

Results

In our dataset, *c.* 32% of the A/C_i curves showed some *TPU* limitation at the upper end of the measurement intercellular CO_2 concentration range (Table 1). Arctic plants and boreal evergreen gymnosperms showed a significantly lower proportion of curves with *TPU*limitation compared to other PFTs (Table 1), while the PFT with the highest proportion of A/C_i curves exhibiting *TPU* limitation was the temperate evergreen angiosperms. We found no detectable correlation between leaf temperature and the C_i at process transition between W_c and W_j, either for the whole dataset or for different PFTs analysed separately (Figure 2a). Similar results were observed for the C_i at the process transition between W_j and W_p (Figure 2b).

The lack of any significant correlations between C_i at process transitions and leaf temperature allowed us to utilise all available data for further inferences. When all data were pooled together, the median intercellular CO_2 concentration at the process transition between W_c and W_j (C_{i-1}) was 423 μmol mol^{-1} (Figure 3a). The median C_i at the process transition between W_j and W_p (C_{i-2}) was 810 μmol mol^{-1} (Figure 3a). Among the different PFTs, Arctic plants showed a significantly higher median C_{i-2} value compared to the others (Figure 3b; *post hoc* Tukey tests, $P < 0.001$). Our data suggested that, at a current ambient atmospheric CO_2 concentration of 400 μmol mol^{-1} (i.e. C_i=280 μmol mol^{-1}; Figure S1b), *c.* 80% of the measured light saturated net photosynthesis values were Rubisco carboxylation (W_c) limited. We did not observe any C_{i-2} values falling below 280 μmol mol^{-1}. Hence, our study suggests *TPU* limitation of light saturated net photosynthesis under current ambient CO_2 concentration is extremely rare. In our dataset, the median of the maximum atmospheric CO_2 concentration set point of A/C_i curve measurements was > 1400 μmol mol^{-1} for all PFTs (Table 1, Figure S1). In all PFTs, the median of the maximum measurement C_i was higher than the median C_i

that *TPU* limitation occurs (i.e. 810 μmol mol^{-1}). Hence, we emphasize that the measurement C_i range was high enough for a robust assessment of *TPU* limitation.

We investigated whether light saturated photosynthetic rates of plants growing in cold environments are more often limited by *TPU* compared to those of plants growing in warmer environments. We observed a weak, but significant negative correlation between the long-term mean growing season air temperature (T_{home}) and the C_i at process transition between W_c and W_j (C_{i-1}; Figure 4a; r^2=0.1). However, we did not detect a significant correlation between T_{home} and the C_i at process transition between W_j and W_p (C_{i-2}; Figure 4b). The lack of a significant correlation between the C_{i-2} and the plants' growth temperature strongly suggests that there is no association between the extent of the *TPU* limitation to light saturated net photosynthesis and home climate.

The instantaneous temperature response of the triose phosphate utilization rate of mature plants growing in their native environments showed distinctly different patterns among the different PFTs. Arctic tundra species showed an exponential increase in *TPU* with increasing leaf temperature, with no optimum temperature within the measured leaf temperature range (Figure 5a). All other PFTs showed a peaked response, where the rate increased up to an optimum temperature and then declined with increasing leaf temperature (Figure 5b-f). The highest optimum temperature for *TPU* was observed for tropical evergreen angiosperms (34.7 °C) and the lowest was observed for the boreal evergreen gymnosperms (28.0 °C). The optimum temperatures for temperate evergreen gymnosperms and temperate evergreen angiosperms were 32.5 and 32.2 °C, respectively (Table 2). The temperature response curves of *TPU* showed a significant departure from the temperature response curves of V_{cmax} (Figure S2). The rate of increase of *TPU* with temperature was shallower than that of V_{cmax} (see Figure S2), so the estimated activation energy of *TPU* was lower than that of V_{cmax} (Table 2). More importantly, in Arctic tundra, both *TPU* and V_{cmax} increased exponentially

with leaf temperature and did not show a temperature optimum within the measurement leaf temperature range (Figure S2a). For other PFTs, the optimum temperature for *TPU* was approximately 6-8°C lower than that for V_{cmax} (Figure S2b-f)

The data showed a significant negative relationship between the basal rate of triose phosphate utilisation at a standard temperature of 25 °C (TPU_{25}) and the long-term mean growing season temperature of the plants' native growth environment (Figure 6a). The highest TPU_{25} was observed for Arctic tundra (30.3±1.6 μmol m^{-2} s^{-1}) and the lowest for tropical evergreen angiosperms (4.7± 0.7 μmol m^{-2} s^{-1}). The ratio between TPU_{25} and the maximum rate of RuBP carboxylation at a standard temperature of 25°C (TPU_{25}:V_{cmax25}) also showed a decreasing trend with increasing long-term mean growing season temperature (T_{home}). Similar to TPU_{25}, the TPU_{25}:V_{cmax25} ratio was highest for the Arctic plants (Figure 6b, Table 2). We developed a simple function to implement this pattern in TBMs (Eqn 7, r^2=0.70). Taken together, these results suggested that the net photosynthetic rate of plants in cold environments is not more frequently *TPU* limited than plants in warmer environments, as the *TPU* is higher for plants in cold environments.

$$\frac{T_{p25}}{V_{cmax25}} = 0.20 - 0.005T_{home} \qquad \text{Eqn 7}$$

Discussion

Our comprehensive analysis of a global dataset of plant photosynthetic CO_2 response measurements across many ecosystems, spanning a measurement temperature range of 3 to 50°C, demonstrates that photosynthesis is not *TPU* limited at current ambient atmospheric CO_2 concentrations. We found no relationship between *TPU* limitation and leaf temperature and there was no evidence to support the view that plants growing in cold environments are more frequently *TPU* limited compared to plants growing in warmer climates. Furthermore, our analysis did not support the common assumption that *TPU* has the same temperature response function as V_{cmax}.

In this study, we demonstrated that light-saturated photosynthesis at current ambient atmospheric CO_2 concentrations (~400 μmol mol^{-1}) is most often Rubisco-limited (80% of the A/C_i curves in our dataset), which agrees with previous work demonstrating that the light-saturated photosynthetic rate at current ambient CO_2 concentration is principally limited by RuBP carboxylation (De Kauwe et al., 2016; Rogers & Humphries, 2000; Yamaguchi et al., 2016). None of the A/C_i curves included in our analysis showed a transition to the *TPU* -limited photosynthetic rate at C_i values less than or equal to 280 μmol mol^{-1}. We can, therefore, be confident that *TPU* rarely limits leaf photosynthesis in natural ecosystems at current ambient atmospheric CO_2 concentrations. Previous work has also shown that *TPU* is rarely reported as a limiting factor for leaf photosynthesis when it is measured under the ambient CO_2 and growth temperatures (Sharkey 1985; Sage & Sharkey, 1987; Yang et al., 2016). Previous studies suggested that plants regulate *TPU* at a rate just slightly higher than what is likely to be required (Yang et al., 2016), but our study indicates that *TPU* limitation is unlikely to be important until CO_2 concentrations reach ~800 μmol mol^{-1}. Further, it has been reported that the *TPU* limitation usually occurs in conditions that are typical for RuBP regeneration limited photosynthesis (Bernacchi et al., 2013). At biologically relevant leaf

temperatures (~1-50°C), RuBP regeneration limitation typically occurs at higher CO_2 partial pressures and mostly at low light levels (von Caemmerer, 2000). Therefore, we conclude that it is rare for photosynthesis to be *TPU* limited under current ambient atmospheric CO_2 concentrations. Furthermore, Free Air CO_2 Enrichment (FACE) experiments where plants are grown at elevated CO_2 concentration in field conditions have demonstrated that V_{cmax} is typically reduced at elevated CO_2 concentration, maintaining Rubisco limitation of light saturated assimilation at elevated CO_2 (Ainsworth & Rogers, 2007). Therefore, it is highly unlikely for photosynthesis to be *TPU* limited under future predicted atmospheric CO_2 concentrations until very high levels are reached.

At low temperatures, the solubility of CO_2, and the specificity of Rubisco for CO_2 relative to O_2, increase, meaning that photorespiration decreases (Jordan & Ogren, 1984). Therefore, the capacity for regeneration of inorganic phosphate (P_i) through photorespiratory metabolism in the chloroplast is decreased because glycolate export from chloroplasts to the peroxisome is reduced (Ellsworth et al., 2015; Harley & Sharkey, 1991; Sharkey, 1985). Additionally, as enzymatic reaction rates associated with the sucrose synthesis are limited at low temperatures (Lambers et al., 2008), accumulation of triose phosphate and PGA in the chloroplast can reduce the regeneration of P_i (Ellsworth et al., 2015; Sharkey, 1985). Hence, it can be hypothesised that net photosynthetic rate could potentially be *TPU* limited in plants grown at low growth temperatures (Labate & Leegood 1988; Lombardozzi et al., 2018; Sharkey, 2016). However, the data presented here clearly refute this hypothesis. We found a significant negative relationship between the basal rate of triose phosphate utilisation at a standard temperature of 25 °C and the long-term mean growing season temperature of the plants' native growth environment. Our data indicate that photosynthesis of plants in cold environments is not more frequently TPU limited than plants in warmer environments, as the TPU is higher for plants in cold environments.

Furthermore, there is evidence that plants have the capacity to compensate for the low temperature-induced decrease in enzyme activity associated with the Calvin cycle, electron transport and sucrose synthesis through several mechanisms including increased concentration of photosynthetic enzymes (Yamori et al., 2005, Yamori et al., 2011), increased expression of cold stable isozymes (Yamori et al., 2006), and maintenance of membrane fluidity (Falcone, Ogas, & Somerville, 2004). Several studies provide evidence for increased concentrations of enzymes associated with sucrose synthesis, including sucrose phosphate synthase and cytosolic fructose-1,6-bisphosphatase (Strand et al., 1997, Strand et al., 1999). These mechanisms may allow cold temperature acclimation of metabolism to alleviate the *TPU* limitation to leaf photosynthesis. Additionally, cold acclimation typically increases the ratio of J_{max}:V_{cmax} (Kattge & Knorr 2007; Kumarathunge et al., 2018a; Rogers et al., 2017b), such that the photosynthetic rate is more likely to be limited by RuBP carboxylation in cold environments. Our data showed that the C_i at the rate transition points from Rubisco carboxylation limitation to RuBP-regeneration limitation was higher than the C_i values corresponding to current ambient CO_2 concentrations for Arctic species. Hence, it is likely that the photosynthetic rate of Arctic species is most frequently RuBP carboxylation limited. Furthermore, Arctic plants have been shown to have a large root to shoot ratio (Iversen et al., 2015), suggesting that sink strength may be sufficient to enable high rates of sucrose export from the leaf and avoid *TPU* limitation (McClain & Sharkey, 2019).

We observed lower activation energies for the instantaneous temperature response of *TPU* compared to V_{cmax} for most PFTs, contradicting the common assumption of similar temperature responses for both processes. Our results contrast with the previous finding by Yang et al. (2016), who reported higher temperature sensitivity of *TPU* compared to V_{cmax}. The activation energies reported in this study were relatively low compared to the values reported by Yang et al. (2016). The temperature response parameters in Yang et al. (2016)

were derived using *TPU* data from different studies where the method of calculating *TPU* (e.g. kinetic constants used in calculations) was not consistent among studies. Hence, our parameter estimates are not directly comparable with those of Yang et al. (2016). Moreover, our results indicate distinct patterning in the basal rate of *TPU* measured at a standard temperature (TPU_{25}) across a climate gradient of long-term mean growing season temperatures. Both TPU_{25} and TPU_{25}:V_{cmax25} were higher for plants growing in cold environments compared to plants in warm environments. The observed pattern for TPU_{25}:V_{cmax25} with T_{home} is consistent with the pattern observed for J_{max}:V_{cmax} at a standard temperature of 25°C at the global scale (Kumarathunge *et al.*, 2019). Taken together, these results suggest that the use of the temperature response function of V_{cmax} to model the temperature response of *TPU*, as implemented in several TBMs, is not correct. Further, our finding of a temperature dependence challenges the use of fixed *TPU*:V_{cmax} ratio in TBMs (Clark et al., 2011; Collatz et al., 1991; Lombardozzi et al., 2018).

Our data demonstrate that the modelled effects of *TPU* limitation on global terrestrial gross primary productivity and the global carbon cycle may not be as large as reported by Lombardozzi et al., (2018), either at current or future projected atmospheric CO_2 concentrations. Lombardozzi et al. (2018) assumed a fixed *TPU*:V_{cmax} ratio, but here we demonstrated that the *TPU*:V_{cmax} ratio decrease with increasing temperature. Further, photosynthetic acclimation to rising CO_2 concentration is not currently implemented in the model used in their study (i.e. CLM4.5). Hence, it is likely that CLM predicts a higher sensitivity to *TPU* at future CO_2 concentrations that is not supported by observations (Ainsworth & Rogers 2007; Leakey et al 2009). We recommend that TBMs should dynamically change *TPU*:V_{cmax} with plants' growth temperature and should use separate temperature response functions to characterize the temperature dependency of *TPU*. Further,

it is necessary to implement photosynthetic acclimation to rising CO_2 concentration in TBMs to improved predictions of GPP in high CO_2 model simulations.

Our global scale synthesis of leaf photosynthesis using measurements obtained from a large number of studies, species, plant functional types and a wide temperature range reveals that the extent of *TPU*limitation at the global scale is uncommon and unrelated to temperature of the growing environment. Taken together, our new formulations of the temperature response of *TPU*should prove useful in quantifying the biochemical limits of terrestrial plant photosynthesis and improving the representation of plant photosynthesis in TBMs.

Acknowledgements

DK was supported by a Western Sydney University international PhD scholarship. AR was supported by the Next-Generation Ecosystem Experiments (NGEE Arctic) project that is supported by the Office of Biological and Environmental Research in the Department of Energy, Office of Science, and through the United States Department of Energy contract No. DE-SC0012704 to Brookhaven National Laboratory. We thank all data contributors for their valuable contribution. We thank Tom Sharkey and an anonymous reviewer for their comments, which served to improve the manuscript.

Author contribution statement

The project was conceived and led by BEM. The analyses were designed and carried out by DPK with guidance from BEM. Manuscript writing was led by DPK and BEM. JED, AR and MGT made substantial contributions to the data interpretation and writing.

References

Ainsworth, E. A., & Rogers, A. (2007). The response of photosynthesis and stomatal conductance to rising [CO_2]: mechanisms and environmental interactions. *Plant, Cell & Environment, 30*(3), 258-270.

Bahar, N. H. A., Hayes, L., Scafaro, A. P., Atkin, O. K., & Evans, J. R. (2018). Mesophyll conductance does not contribute to greater photosynthetic rate per unit nitrogen in temperate compared with tropical evergreen wet-forest tree leaves. *New Phytologist*, 218: 492-505.

Bernacchi, C. J., Bagley, J. E., Serbin, S. P., Ruiz-Vera, U. M., Rosenthal, D. M., & Vanloocke, A. (2013). Modelling C3 photosynthesis from the chloroplast to the ecosystem. *Plant, Cell & Environment, 36*(9), 1641-1657.

Bernacchi, C. J., Singsaas, E. L., Pimentel, C., Portis Jr, A. R., & Long, S. P. (2001). Improved temperature response functions for models of Rubisco-limited photosynthesis. *Plant, Cell & Environment, 24*(2), 253-259.

Busch, F. A., & Sage, R. F. (2017). The sensitivity of photosynthesis to O_2 and CO_2 concentration identifies strong Rubisco control above the thermal optimum. *New Phytologist, 213*(3), 1036-1051.

Von Caemmerer, S. (2013). Steady-state models of photosynthesis. *Plant, Cell & Environment, 36*(9), 1617-1630.

Clark, D. B., Mercado, L. M., Sitch, S., Jones, C. D., Gedney, N., Best, M. J., . . . Cox, P. M. (2011). The Joint UK Land Environment Simulator (JULES), model description – Part 2: Carbon fluxes and vegetation dynamics. *Geoscientific Model Development, 4*(3), 701-722.

Collatz, G. J., Ball, J. T., Grivet, C., & Berry, J. A. (1991). Physiological and environmental regulation of stomatal conductance, photosynthesis and transpiration: a model that includes a laminar boundary layer. *Agricultural and Forest Meteorology, 54*(2), 107-136.

Crous, K. Y., Quentin, A. G., Lin, Y. S., Medlyn, B. E., Williams, D. G., Barton, C. V., & Ellsworth, D. S. (2013). Photosynthesis of temperate Eucalyptus globulus trees outside their native range has limited adjustment to elevated CO2 and climate warming. *Glob Chang Biol, 19*(12), 3790-3807.

De Kauwe, M. G., Lin, Y.-S., Wright, I. J., Medlyn, B. E., Crous, K. Y., Ellsworth, D. S., . . . Domingues, T. F. (2016). A test of the 'one-point method' for estimating maximum carboxylation capacity from field-measured, light-saturated photosynthesis. *New Phytologist, 210*(3), 1130-1144.

Dreyer, E., Le Roux, X., Montpied, P., Daudet, F. A., & Masson, F. (2001). Temperature response of leaf photosynthetic capacity in seedlings from seven temperate tree species. *Tree Physiology, 21*(4), 223-232.

Duursma, R. A. (2015). Plantecophys - An R Package for Analysing and Modelling Leaf Gas Exchange Data. *PLoS ONE, 10*(11), e0143346.

Ellsworth, D. S., Crous, K. Y., Lambers, H., & Cooke, J. (2015). Phosphorus recycling in photorespiration maintains high photosynthetic capacity in woody species. *Plant, Cell & Environment, 38*(6), 1142-1156.

Falcone, D. L., Ogas, J. P., & Somerville, C. R. (2004). Regulation of membrane fatty acid composition by temperature in mutants of Arabidopsis with alterations in membrane lipid composition. *BMC Plant Biology, 4*(1), 17.

Farquhar, G. D., von Caemmerer, S., & Berry, J. A. (1980). A biochemical model of photosynthetic CO2 assimilation in leaves of C3 species. *Planta, 149*(1), 78-90.

Gu, L., Pallardy, S. G., Tu, K., Law, B. E., & Wullschleger, S. D. (2010). Reliable estimation of biochemical parameters from C_3 leaf photosynthesis–intercellular carbon dioxide response curves. *Plant, Cell & Environment, 33*(11), 1852-1874.

Harley, P. C., & Sharkey, T. D. (1991). An improved model of C_3 photosynthesis at high CO2: Reversed O2 sensitivity explained by lack of glycerate re-entry into the chloroplast. *Photosynthesis Research, 27*(3), 169-178.

Hijmans, R. J., Cameron, S. E., Parra, J. L., Jones, P. G., & Jarvis, A. (2005). Very high resolution interpolated climate surfaces for global land areas. *International Journal of Climatology, 25*(15), 1965-1978.

Hikosaka, K., Ishikawa, K., Borjigidai, A., Muller, O., & Onoda, Y. (2006). Temperature acclimation of photosynthesis: mechanisms involved in the changes in temperature dependence of photosynthetic rate. *Journal of Experimental Botany, 57*(2), 291-302.

Iversen, C. M., Sloan, V. L., Sullivan, P. F., Euskirchen, E. S., McGuire, A. D., Norby, R. J., . . . Wullschleger, S. D. (2015). The unseen iceberg: plant roots in arctic tundra. *New Phytologist, 205*(1), 34-58.

Johnson FH, Eyring H, Williams RW (1942) The nature of enzyme inhibitions in bacterial luminescence: Sulfanilamide, urethane, temperature and pressure. Journal of Cellular and Comparative Physiology, **20**, 247-268.

Jordan, D. B., & Ogren, W. L. (1984). The CO_2/O_2 specificity of ribulose 1,5-bisphosphate carboxylase/oxygenase. *Planta, 161*(4), 308-313.

Kattge, J., & Knorr, W. (2007). Temperature acclimation in a biochemical model of photosynthesis: a reanalysis of data from 36 species. *Plant, Cell & Environment, 30*(9), 1176-1190.

Kattge, J., Knorr, W., Raddatz, T., & Wirth, C. (2009). Quantifying photosynthetic capacity and its relationship to leaf nitrogen content for global-scale terrestrial biosphere models. *Global Change Biology, 15*(4), 976-991.

Kumarathunge DP, Medlyn BE, Drake JE *et al.* (2019) Acclimation and adaptation components of the temperature dependence of plant photosynthesis at the global scale. New Phytologist, 222, 768-784.

Kumarathunge, D. P., Medlyn, B. E., Drake, J. E., Tjoelker, M. G., Aspinwall, M. J., Battaglia, M., . . . Danielle, A. W. (2018). ACi-TGlob_V1.0: A Global dataset of photosynthetic CO_2 response curves of terrestrial plants. doi:10.6084/m9.figshare.7283567.v1

Labate, C. A., & Leegood, R. C. (1988). Limitation of photosynthesis by changes in temperature. *Planta, 173*(4), 519-527.

Lombardozzi, D., Nicholas, G. S., Susan, J. C., Jeffrey, S. D., Thomas, D. S., Alistair, R., . . . Gordon, B. B. (2018). Triose phosphate limitation in photosynthesis models reduces leaf photosynthesis and global terrestrial carbon storage. *Environmental Research Letters, 13*(7), 074025.

Mcclain AM, Sharkey TD (2019) Triose phosphate utilization and beyond: from photosynthesis to end product synthesis. Journal of Experimental Botany, 70, 1755-1766.

Manter, D. K., & Kerrigan, J. (2004). A/C_i curve analysis across a range of woody plant species: influence of regression analysis parameters and mesophyll conductance. *Journal of Experimental Botany, 55*(408), 2581-2588.

Medlyn, B. E., Dreyer, E., Ellsworth, D., Forstreuter, M., Harley, P. C., Kirschbaum, M. U. F., . . . Loustau, D. (2002). Temperature response of parameters of a biochemically based model of photosynthesis. II. A review of experimental data. *Plant, Cell & Environment, 25*(9), 1167-1179.

Medlyn, B. E., Duursma, R. A., & Zeppel, M. J. B. (2011). Forest productivity under climate change: a checklist for evaluating model studies. *Wiley Interdisciplinary Reviews: Climate Change, 2*(3), 332-355.

Mercado, L. M., Medlyn, B. E., Huntingford, C., Oliver, R. J., Clark, D. B., Stephen, S., . . . Cox, P. M. (2018). Large sensitivity in land carbon storage due to geographical and temporal variation in the thermal response of photosynthetic capacity. *New Phytologist, 218*(4), 1462-1477.

Pons, T L. (2012). Interaction of temperature and irradiance effects on photosynthetic acclimation in two accessions of arabidopsis thaliana. *Photosynthesis Research.*, 113 (1), 207-219.

Rigby, R. A., & Stasinopoulos, D. M. (2005). Generalized additive models for location, scale and shape. *Journal of the Royal Statistical Society: Series C (Applied Statistics), 54*(3), 507-554.

Rogers, A., & Humphries, S. W. (2000). A mechanistic evaluation of photosynthetic acclimation at elevated CO2. *Global Change Biology, 6*(8), 1005-1011.

Rogers, A., Medlyn, B. E., Dukes, J. S., Bonan, G., von Caemmerer, S., Dietze, M. C., . . . Zaehle, S. (2017). A roadmap for improving the representation of photosynthesis in Earth system models. *New Phytologist, 213*(1), 22-42.

Rogers, A., Serbin, S. P., Ely, K. S., Sloan, V. L., & Wullschleger, S. D. (2017). Terrestrial biosphere models underestimate photosynthetic capacity and CO_2 assimilation in the Arctic. *New Phytologist, 216*(4), 1090-1103.

Sage, R. F., & Sharkey, T. D. (1987). The Effect of Temperature on the Occurrence of O_2 and CO_2 Insensitive Photosynthesis in Field Grown Plants. *Plant Physiology, 84*(3), 658-664.

Sage, R. F., Sharkey, T. D., & Seemann, J. R. (1989). Acclimation of Photosynthesis to Elevated CO_2 in Five C_3 Species. *Plant Physiology, 89*(2), 590-596.

Sharkey, T. D. (1985). Photosynthesis in intact leaves of C_3 plants: Physics, physiology and rate limitations. *The Botanical Review, 51*(1), 53-105.

Sharkey TD, Stitt M, Heineke D, Gerhardt R, Raschke K, Heldt HW (1986) Limitation of Photosynthesis by Carbon Metabolism II. O_2-Insensitive CO_2 Uptake Results from Limitation Of Triose Phosphate Utilization*,* 81, 1123-1129.

Sharkey, T. D. (2016). What gas exchange data can tell us about photosynthesis. *Plant, Cell & Environment, 39*(6), 1161-1163.

Sharkey, T. D., Bernacchi, C. J., Farquhar, G. D., & Singsaas, E. L. (2007). Fitting photosynthetic carbon dioxide response curves for C3 leaves. *Plant, Cell & Environment, 30*(9), 1035-1040.

Smith, N. G., & Dukes, J. S. (2013). Plant respiration and photosynthesis in global-scale models: incorporating acclimation to temperature and CO2. *Global Change Biology, 19*(1), 45-63.

Smith, N. G., Lombardozzi, D., Tawfik, A., Bonan, G., & Dukes, J. S. (2017). Biophysical consequences of photosynthetic temperature acclimation for climate. *Journal of Advances in Modeling Earth Systems, 9*(1), 536-547.

Smith, N. G., Malyshev, S. L., Shevliakova, E., Kattge, J., & Dukes, J. S. (2016). Foliar temperature acclimation reduces simulated carbon sensitivity to climate. *Nature Clim. Change, 6*(4), 407-411.

Stitt, M., & Hurry, V. (2002). A plant for all seasons: alterations in photosynthetic carbon metabolism during cold acclimation in Arabidopsis. *Current Opinion in Plant Biology, 5*(3), 199-206.

Stitt M, Grosse H (1988) Interactions between Sucrose Synthesis and CO2 Fixation IV. Temperature-dependent adjustment of the relation between sucrose synthesis and CO2 fixation. Journal of Plant Physiology, **133**, 392-400.

Stitt M, Grosse H, Woo K-C (1988) Interactions between Sucrose Synthesis and CO2 Fixation II. Alterations of Fructose 2,6-bisphosphate during Photosynthetic Oscillations. Journal of Plant Physiology, **133**, 138-143.

Strand, Å., Hurry, V., Gustafsson, P., & Gardeström, P. (1997). Development of Arabidopsis thaliana leaves at low temperatures releases the suppression of photosynthesis and photosynthetic gene expression despite the accumulation of soluble carbohydrates. *The Plant Journal, 12*(3), 605-614.

Strand, Å., Hurry, V., Henkes, S., Huner, N., Gustafsson, P., Gardeström, P., & Stitt, M. (1999). Acclimation of Arabidopsis Leaves Developing at Low Temperatures. Increasing Cytoplasmic Volume Accompanies Increased Activities of Enzymes in the Calvin Cycle and in the Sucrose-Biosynthesis Pathway. *Plant Physiology, 119*(4), 1387-1398.

Yang, J. T., Preiser, A. L., Li, Z., Weise, S. E., & Sharkey, T. D. (2016). Triose phosphate use limitation of photosynthesis: short-term and long-term effects. *Planta, 243*(3), 687-698.

Table 1. Descriptive statistics of triose phosphate utilization rate limitation across different plant functional types.

Plant Functional Type	Total number of datasets	Total number of species	Total number of A/C_i curves	Measured maximum intercellular CO_2 concentration (μmol mol^{-1})†	Maximum atmospheric CO_2 concentration set point of individual A/C_i curves (μmol mol^{-1})†	Number of A/C_i curves showing *TPU* limitation‡
Arctic tundra	1	7	242	1531 (1340 – 1746)	1786 (1772 – 1915)	30 (12%)
Boreal evergreen gymnosperms	5	4	429	1348 (929 – 1685)	1800 (1601 – 1973)	71 (17%)
Temperate evergreen gymnosperms	7	10	672	1496 (1220 – 1839)	1778 (1102 – 1909)	134 (20%)
Temperate deciduous angiosperms	11	17	1011	1030 (897 – 1832)	1481 (1465 – 1529)	335 (33%)
Temperate evergreen angiosperms	13	27	1253	1362 (1039 – 1744)	1767 (1747 – 1981)	591(47%)
Tropical evergreen angiosperms	6	47	653	1227 (896 – 1811)	1747 (1193 – 1979)	209 (32%)
Whole dataset	43	112	4260	1283 (957 – 1820)	1783 (1524 – 1993)	1370 (32%)

†Values given are the median (2.5th and 97.5th percentiles of the distribution)

‡Within the measurement C_i range of a given A/C_i curve.

Table 2. Temperature response parameters of *TPU* and V_{cmax} for mature plants growing in their native environments.

Plant Functional Type	Basal rate at 25°C (μmol $m^{-2}s^{-1}$)		E_a (kJ mol^{-1})		ΔS (J $mol^{-1}K^{-1}$)		T_{opt} (°C)	
	TPU	V_{cmax}	*TPU*	V_{cmax}	*TPU*	V_{cmax}	*TPU*	V_{cmax}
Arctic tundra	20.3 (1.6)	78.3 (12.7)	46.2 (5.3)	55.9 (4.8)	Not estimated	657.5 (5.7)	Not estimated	26.7
Boreal evergreen gymnosperms	7.9 (1.4)	80.4 (8.0)	30.9 (10.4)	50.3 (4.7)	650 (3.8)	637.6 (3.2)	28.0	36.1
Temperate evergreen gymnosperms	6.0 (0.9)	42.8 (13.9)	36.5 (5.6)	60.1 (7.7)	642 (4.1)	635.2 (5.6)	32.5	38.3
Temperate deciduous angiosperms	9.0 (2.1)	39.0 (1.4)	28.8 (10.6)	69.0 (3.8)	644 (3.1)	636.6 (1.7)	30.4	38.4
Temperate evergreen angiosperms	8.7 (1.0)	82.9 (11.0)	23.7 (6.1)	86.4 (4.6)	638 (3.1)	632.4 (1.7)	32.2	39.5
Tropical evergreen angiosperms	4.7 (0.7)	39.4 (8.9)	53.9 (13.8)	47.4 (10.0)	641 (3.5)	623.1 (9.1)	34.7	44.3

TPU is the triose phosphate utilisation rate, V_{cmax} is the maximum rate of RuBP carboxylation, E_a is the activation energy, ΔS is the entropy and T_{opt} is the optimum temperature. Except for Arctic tundra, a peaked Arrhenius model was used to parameterise the instantaneous temperature response. For Arctic tundra, *TPU* exponentially increased within the measurement leaf temperature range, hence the standard Arrhenius model was fitted to the data.

Do not distribute

Figure legends

Figure 1. Conceptual figure demonstrating the typical CO_2 response of leaf net photosynthesis (A/C_i curve). Filled circles depict the measured leaf net photosynthetic rated at different intercellular CO_2 concentration levels (C_i). Solid lines depict the Rubisco carboxylation limited photosynthetic rate (W_c limitation, purple line), RuBP-regeneration limited photosynthetic rate (W_j limitation, orange line), triose phosphate utilization limited rate (W_p limitation, gray line) and the limiting rate of net photosynthesis (black). The two filled circles depict the C_i at transition points from Rubisco carboxylation limited photosynthetic rate to RuBP-regeneration limited photosynthetic rate (C_{i-1}, purple circle) and from RuBP-regeneration limited photosynthetic rate to *TPU* limited photosynthetic rate (C_{i-2}, orange circle). The dashed and dotted lines depict the CO_2 supply functions corresponding to current ambient CO_2 concentration (400 μmol mol^{-1}, dashed line) and an elevated CO_2 concentration (600 μmol mol^{-1}, dotted line). The background shaded area depicts the C_i range where net photosynthesis is limited by W_c (purple), W_j (orange) and W_p (gray). The data shown in this figure was obtained at a leaf measurement temperature of 18 °C on *Eucalyptus parramattensis* trees grown in whole tree chambers in Richmond NSW Australia. The fitted parameter values were V_{cmax}= 155, J_{max}=250, *TPU* =11 and R_{day}=3.1 μmol m^{-2} s^{-1}.

Figure 2. The intercellular CO_2 concentration at rate transition points as a function of leaf temperature. Panel (a) depicts the C_i at the rate transition point from Rubisco-limited photosynthesis to RuBP-regeneration-limited photosynthesis (C_{i-1}). Panel (b) depicts the C_i at rate transition point from RuBP-regeneration-limited photosynthesis to *TPU* limited photosynthesis (C_{i-2}). Filled symbols show the mean of data binned in 1°C increments and the original data are shown in the background with unfilled symbols. The horizontal broken line

depicts the C_i value corresponding to current ambient atmospheric CO_2 concentration (~400 μmol mol^{-1}) at a C_i:C_a ratio of 0.7. The legend in panel (a) depicts six different plant functional types, Arctic tundra, Temperate deciduous angiosperms (Te-DA), Temperate evergreen angiosperms (Te-EA), Tropical evergreen angiosperms (Tr-EA), Boreal evergreen gymnosperms (Br-EG), Temperate evergreen gymnosperms (Te-EG). Note the data shown here are from the A/C_i curves which showed *TPU* limitation within the measurement C_i range (*n*=1114)

Figure 3. The distribution of intercellular CO_2 concentration at the rate transition point. In panel (a) the shaded area depicts the distribution of C_i at the rate transition point from Rubisco carboxylation limited photosynthetic rate to RuBP-regeneration limited photosynthetic rate (gray) and from RuBP-regeneration limited photosynthetic rate to *TPU* limited photosynthetic rate (pink). The thick vertical lines in respective colours in panel (a) show the median C_i for the two transition steps and the dashed line depicts the Ci value corresponding to the current ambient atmospheric CO_2 level (~400 μmol mol^{-1}) at a C_i:C_a of 0.7. Panel (b) shows the C_i value at the transition point from RuBP regeneration limited photosynthesis to *TPU* limited photosynthesis for six different plant functional types, Arctic tundra, Temperate deciduous angiosperms (Te-DA), Temperate evergreen angiosperms (Te-EA), Tropical evergreen angiosperms (Tr-EA), Boreal evergreen gymnosperms (Br-EG), Temperate evergreen gymnosperms (Te-EG). In the boxplots, the thick black line and box depict the median and interquartile range respectively, with bars extending to 1.5 times the interquartile range. Dots outside of the box and whiskers show outlying data points.

Figure 4. Intercellular CO_2 concentration at rate the transition point at a standard temperature of 25°C, as a function of climate of the growing environment for various plant functional types. Panel (a) depicts the Ci at the rate transition point from Rubisco carboxylation limited photosynthetic rate to RuBP-regeneration limited photosynthesis and panel (b) depicts the Ci at rate transition point from RuBP-regeneration limited photosynthetic rate to *TPU* limited photosynthetic rate. The dashed lines in each panel depicts the Ci value corresponding to the current ambient atmospheric CO_2 level (~400 μmol mol^{-1}) at a C_i:C_a of 0.7. The thick line in panel (a) depicts the least-squares linear regression fit ($y = 499.6 - 9.4x$; r^2=0.1) and the shaded area shows the 95% CI of predictions. The data presented here are measurements of mature plants grown and measured in their native environments for different plant functional types, Arctic tundra, Temperate deciduous angiosperms (Te-DA), Temperate evergreen angiosperms (Te-EA), Tropical evergreen angiosperms (Tr-EA), Boreal evergreen gymnosperms (Br-EG), Temperate evergreen gymnosperms (Te-EG). T_{home} is the mean (1960-1996) growing season air temperature (i.e. mean temperature of the months with mean temperatures above 0 °C).

Figure 5. Instantaneous temperature response of the triose phosphate utilisation rate (*TPU*) of mature plants growing in their native environments for different plant functional types, (a) Arctic tundra, (b) Boreal evergreen gymnosperms (Br-EG), (c) Temperate evergreen gymnosperms (Te-EG), (d) Temperate deciduous angiosperms (Te-DA), (e) Temperate evergreen angiosperms (Te-EA), (f) Tropical evergreen angiosperms (Tr-EA). Filled circles depict the *TPU* values from fitting Eqn 4 to A/Ci curves (only A/C_i curves which showed *TPU* limitation within the measurement C_i range, n=1114). Lines in each panel show the fitted standard Arrhenius model (in panel a) or the peaked Arrhenius model (in panels b-f). Fitted temperature response parameters are given in Table 2. Note the disparity in x-axis scales.

Figure 6. Rate of triose phosphate utilisation at a standard temperature of 25°C (TPU_{25}; panel a) and the TPU_{25}:V_{cmax25} ratio of mature plants growing in their native environments. Lines in each panel show fitted generalised additive models. Shaded area shows the 95% CI of predictions. Legend in panel (a) depict plant functional types; Arctic tundra, Temperate deciduous angiosperms (Te-DA), Temperate evergreen angiosperms (Te-EA), Tropical evergreen angiosperms (Tr-EA), Boreal evergreen gymnosperms (Br-EG), Temperate evergreen gymnosperms (Te-EG). T_{home} is the mean (1960-1996) growing season air temperature (i.e. mean temperature of the months with mean temperatures above 0 °C) at species' growing environment. Error bars represent ±1SE.

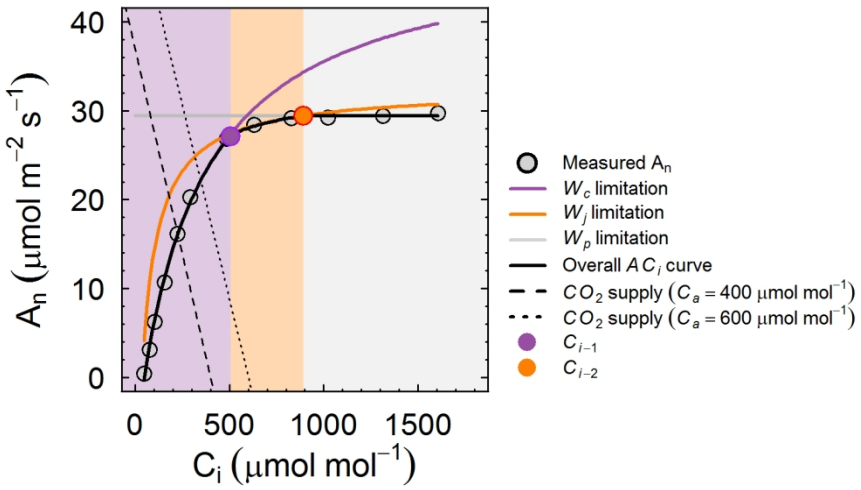

Figure 1

152x76mm (300 x 300 DPI)

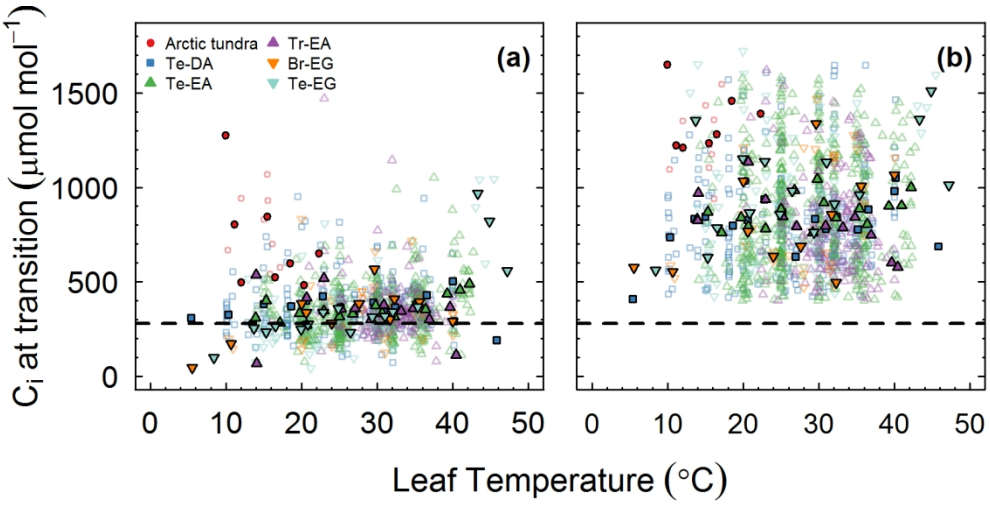

Figure 2

152x76mm (300 x 300 DPI)

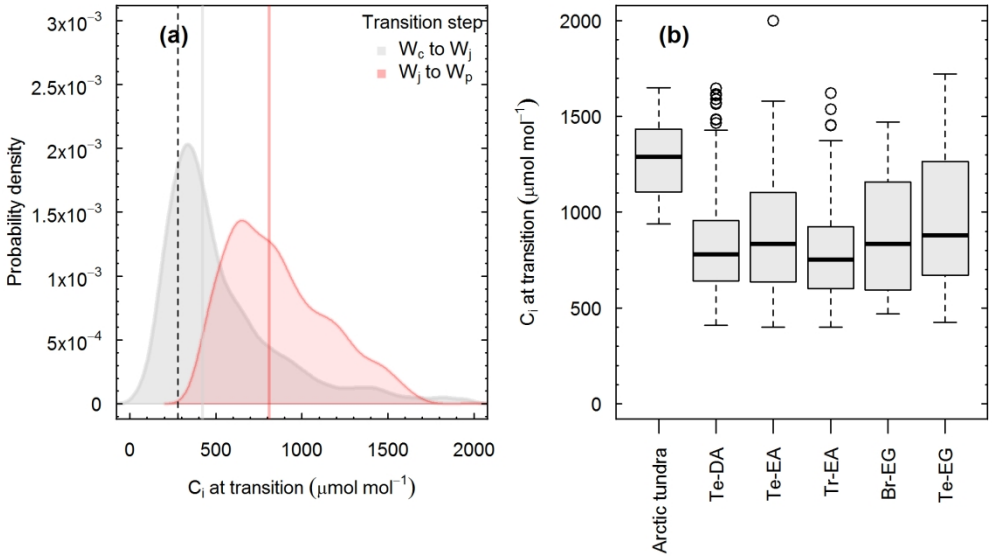

Figure 3

177x101mm (300 x 300 DPI)

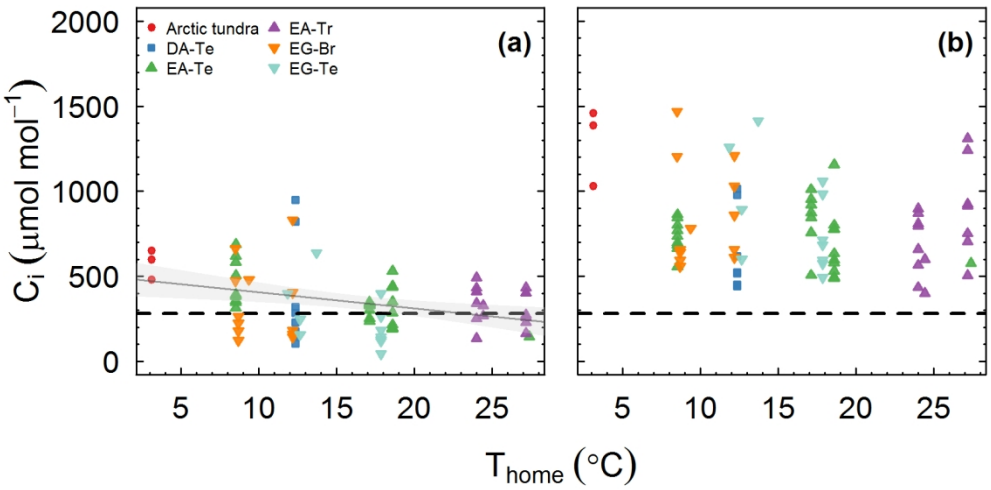

Figure 4

152x76mm (300 x 300 DPI)

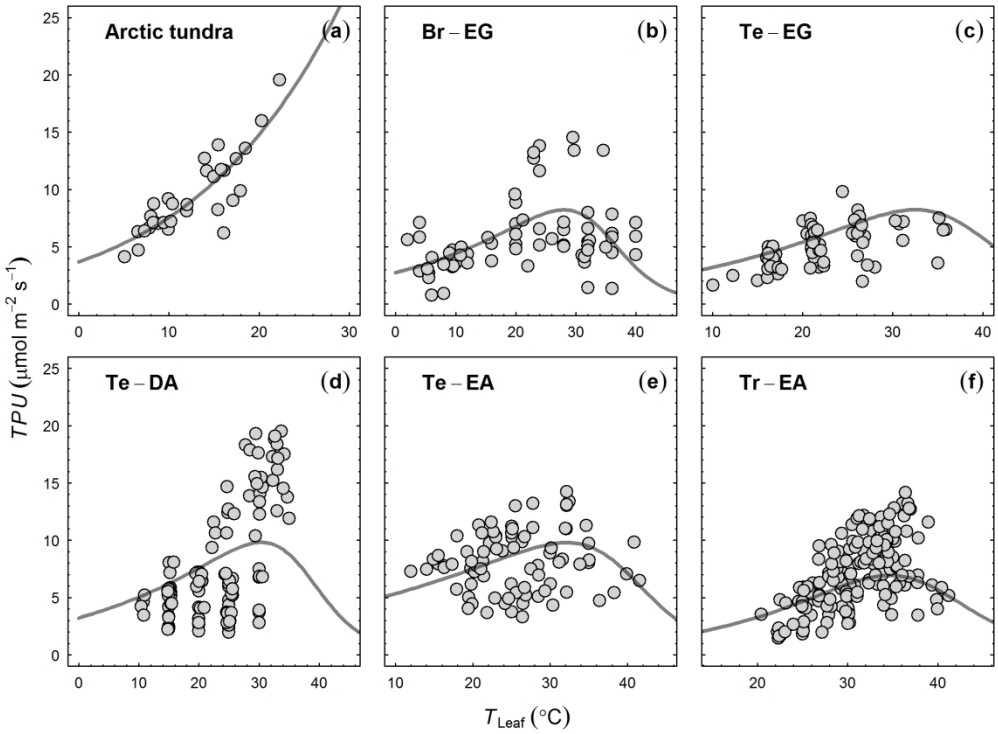

Figure 5

203x152mm (300 x 300 DPI)

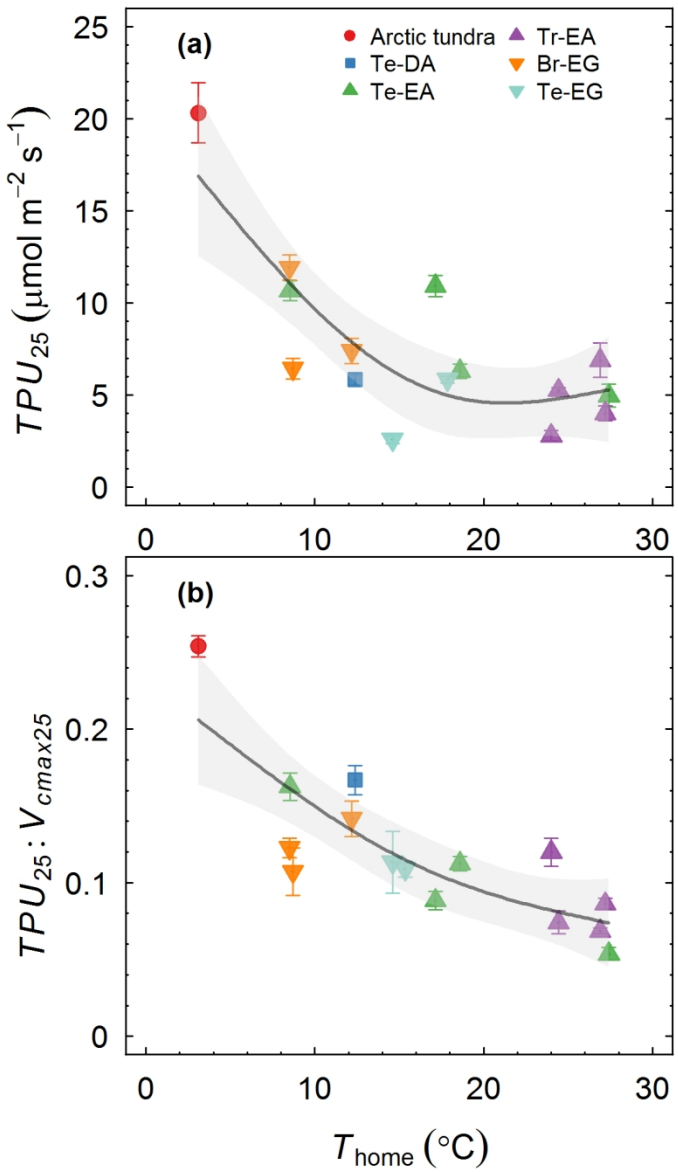

Figure 6

101x177mm (300 x 300 DPI)

Summary statement

We demonstrate that triose phosphate utilization rate does not limit leaf photosynthesis at the current ambient atmospheric CO_2 concentration. Our results do not support the hypothesis that the light saturated photosynthetic rates of plants growing in cold environments are more often limited by triose phosphate utilization rate than those of plants growing in warmer environments. In addition, we showed that instantaneous temperature responses of triose phosphate utilization rate are distinct from temperature responses of the maximum rate of Rubisco carboxylation.

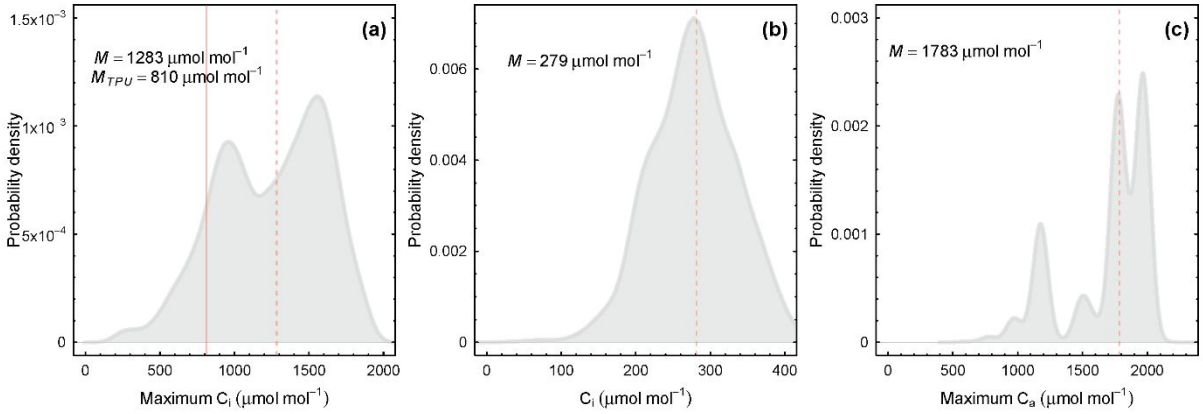

Figure S1. Distribution of (a) measured maximum intercellular CO_2 concentration (C_i) of individual AC_i curves (*n*=4260), (b) C_i at the current ambient CO_2 concentration of 400 μmol mol^{-1} (*n*=7269) and (c) maximum atmospheric CO_2 concentration (C_a) set point of individual AC_i curves (*n*=4183). In panel (a), continuous vertical line depicts the median C_i at process transition between RuBP-regeneration limited photosynthetic rate to T_P limited photosynthetic rate (M_{TPU}) and the dashed line depicts the median maximum C_i of the distribution (M). In panels (b) and (c), the dash line depicts the median (M) of the distribution. Note in some A/C_i curves, there were multiple measurements at ambient CO_2 levels. Hence the number of data points at ambient CO_2 level was higher than the number of A/C_i curves.

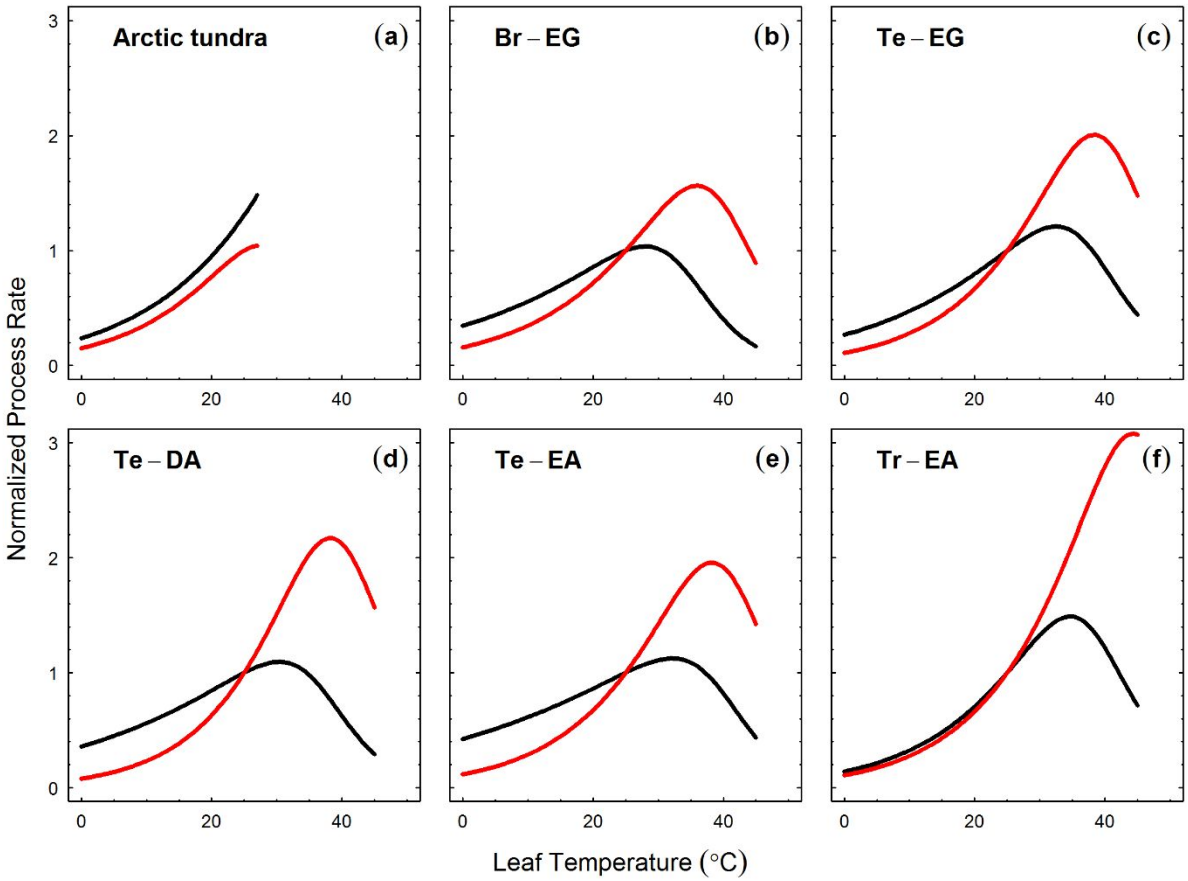

Figure S2. Instantaneous temperature response of the rate of triose phosphate utilisation rate (*TPU*; black) and the maximum rate of ribulose-1,5-bisphosphate carboxylase-oxygenase (Rubisco) activity (V_{cmax}; red) of mature plants growing in their native environments for different plant functional types, Arctic tundra, Boreal evergreen gymnosperms (Br-EG), Temperate evergreen gymnosperms (Te-EG), Temperate deciduous angiosperms (Te-DA), Temperate evergreen angiosperms (Te-EA), Tropical evergreen angiosperms (Tr-EA). Data shown here are the standardised to values at 25°C.

Table S1. List of species, seed source location and measurement settings. Treatments column shows specific growth temperature, growth CO_2 concentration and watering treatments whenever implemented in different datasets. We recommend users to refer to the original publications given for each datasets for more detailed explanation on different treatments. Unless specially mentioned, plants were grown under natural light conditions. In datasets where specific treatments not implemented, plants were grown under natural environmental conditions of the experimental site

Dataset	Species	Seed source location		Measurement PPFD (µmol $m^{-2}s^{-1}$)	Measurement temperature range (°C)	Growth temperature range (°C)	Treatments	Data collection periods	Age of plants	Data type	Reference
		latitude	longitude								
Dillaway DBF spp, USA-IL	*Betula papyrifera* *Liquidambar styraciflua* *Populus deltoides* *Populus tremuloides*	45.0 38.0 43.0 43.0	-89.0 -84.0 -89.0 -89.0	1800	21 – 37	30.6	Natural environmental conditions	August 2007	saplings	ACi-T	Dillaway and Kruger (2010)
Dillaway DBF spp, USW-WI (N)	*Betula papyrifera,* *Liquidambar styraciflua,* *Populus deltoides,* *Populus tremuloides*	45.0 38.0 43.0 43.0	-89.0 -84.0 -89.0 -89.0	1800	21 – 37	18.7	Natural environmental conditions	August 2007	saplings	ACi-T	Dillaway and Kruger (2010)
Dillaway DBF spp, USW-WI (S)	*Betula papyrifera,* *Liquidambar styraciflua,* *Populus deltoides,* *Populus tremuloides*	45.0 38.0 43.0 43.0	-89.0 -84.0 -89.0 -89.0	1800	21-37	22.5	Natural environmental conditions	August 2007	saplings	ACi-T	Dillaway and Kruger (2010)
Lin Eucalypt spp, AU-NSW	*Eucalyptus cladocalyx* *Eucalyptus crebra* *Eucalyptus dunnii* *Eucalyptus melliodora* *Eucalyptus saligna* *Eucalyptus tereticornis*	-33.03 -33.61 -28.41 -35.11 -30.37 -30.04	138.75 150.81 153.02 147.37 152.10 150.73	1500	15 – 36	8.8 – 25.3	Natural environmental conditions	August 2008 November 2008 February 2009	saplings	ACi-T An-T	Lin *et al.* (2013)
Vårhammar EBF spp, Rwanda	*Carapa procera,* *Entandrophragma excelsum* *Hagenia abyssinica,* *Cedrela serrata,* *Eucalyptus maidenii* *Eucalyptus microcorys*	-2.47 -2.47 -2.47 34.08 -36.56 -30.58	29.20 29.20 29.20 73.47 149.65 152.62	1800	20 – 40	19.4	Natural environmental conditions	July – August 2011	saplings	ACi-T	Vårhammar *et al.* (2015)
Rainforest understory, Puerto Rico	*Prestoea montana* *Psychotria brachiate* *Piper glabrescens* *Rourea surinamensis* *Miconia prasina*	18.18	-65.73	800	20 – 40	24.0	Natural environmental conditions	March – August 2014	mature	ACi-T	Alida C. Mau and Molly A. Cavaleri Unpublished data
Black Spruce, USA-MN	*Picea mariana*	47.50	-93.45	1700	2 – 50	5.3 – 17.5	Natural environmental conditions	June, September 2010 July, October 2011 May, June, October 2012 April, July, August 2013	mature	ACi-T	Jensen *et al.* (2015)
Arctic tundra, USA-AK	*Arctagrostis latifolia* *Arctophila fulva*	71.28	-156.65	2000	5 – 25	3.1	Natural environmental conditions	July, August 2012 July 2013	mature	ACi-T	Rogers *et al.* (2017)

	Dupontia fisheri *Carex aquatilis* *Eriophorum angustifolium* *Petasites frigidus* *Salix pulchra*							July 2014 July 2015			
Loblolly Pine, US-NC	*Pinus taeda*	35.96	-79.08	1800	10 – 35	11.8 – 26.4	Natural environmental conditions	December 1998 August 1999	mature	ACi-T	David Ellsworth, Unpublished data
Eucalypt Woodland, AU-NSW	*Eucalyptus tereticornis*	-33.62	150.74	1800	25 – 42	17.1	Natural environmental conditions		mature	ACi-T	Crous and Ellsworth, Unpublished data
Semi-arid Woodland, AU-WA	*Eucalyptus clelandii* *E. salmonophloia* *E. salubris,* *E. transcontinentalis,* *Eremophila scoparia,* *Acacia aneura,* *Acacia. hemiteles* *Callitris columellaris*	-30.19	120.65	1800	20 – 35	21.9	Natural environmental conditions	March-April 2013 August-September 2013	mature	ACi-T	Fürstenau Togashi *et al.* (2017)
Hinoki Cypress, Japan	*Chamaecyparis obtusa*	36.05	140.11	1100	15 – 30	11.9	Natural environmental conditions	April 2004 October 2004	seedlings	ACi-T	Han *et al.* (2006)
Japanese Beech, Japan	*Fagus crenata*	40.63	140.85	1000 - 2000	15 – 35	15.9 – 25.3	Natural environmental conditions	May 2002 August 2002 October 2002	seedlings	ACi-T	Onoda *et al.* (2005)
Red Pine, Japan	*Pinus densiflora*	35.45	138.8	1100	15 – 30	11.8	Natural environmental conditions	May 2001 July 2001 November 2001	mature	ACi-T	Han *et al.* (2004)
Tropical forest, Puerto Rico	*Dacryodes excels* *Castilla elastica*	18.31	-65.73	600 - 800	20 – 35	24.0	Natural environmental conditions	July 2015	mature	ACi-T	Kelsey R. Carter and Molly A. Cavaleri Unpublished data
Rainforest, Panama (A)	Calophyllum longifolium Ficus insipida Garcinia madruno Lagerstroemia speciose	8.99	-79.54	1500	22 – 42	26.9	Natural environmental conditions	November 2016 – January 2017	mature	ACi-T	Slot and Winter (2017)
Rainforest, Panama (B)	*Anacardium excelsum* *Apeiba membranacea* *Brosimum utile* *Carapa guianensis* *Cordia bicolor* *Garcinia madruno* *Guatteria dumetorum* *Manilkara bidentate* *Miconia minutiflora* *Protium panamense* *Simarouba amara* *Tachigali versicolor* *Tapirira guianensis* *Terminalia amazonia*	8.99	-79.54				Natural environmental conditions			An-T	Slot and Winter (2017)

	Tocoyena pittieri *Vantanea depleta* *Virola multiflora* *Vochysia ferruginea* *Astronium graveolens* *Castilla elastica* *Cecropia peltata* *Chrysophyllum cainito* *Ficus insipida* *Luehea seemannii* *Macrocnemum roseum* *Nectandra cuspidata* *Pittoniotis trichantha* *Schefflera morototoni* *Spondias mombin* *Zuelania guidonia*									
Maritime Pine, France	*Pinus pinaster* prov. Landes prov. Tamjout	44.0 0.58 35.14 5.25	1400	15 – 35	6.7 – 20.9	Natural environmental conditions	July 1999 September 1999 November 1999 January 2000 March 2000 June 2000 October 2000	mature	ACi-T	Medlyn *et al.* (2002)
Mongolian Oak, Japan	*Quercus crispula*	42.66 141.6	1000	10 - 30	12.3 – 17.5	Natural environmental conditions	June 2001 August 2001 September 2001 June 2002 August 2002 September 2002	mature	ACi-T	Hikosaka *et al.* (2007)
Rainforest, Brazil	*Peltogine excels* *Protium sp* *Ocotea sp.* *Diospyrus praetermissa* *Tachigali mimercophyla* *Jacaranda copaia* *Licania micheli* *Ocotea sp.* *Quaruba branca* *Miratinga perebea* *Bertholletia excels* *Tetragastris panamensis* *Crysophillum sp.* *Abuta panurensis* *Macherium sp.* *Tetracera amazonica* *Brosimum parinarioides* *Guarea sp.*	-2.63 -60.12	NA	25 – 42	25.8 – 27.8	Natural environmental conditions	June – November 2001 March 2004	mature	ACi-T	Tribuzy (2005)

	Pouteria erythrochrysa *Pouteria anomala* *Couepia longipondula* *Micropholis guyanensis* *Eschweilera coriacea* *Bellucia dichotoma* *Zygia racemosa* *Pouteria williamii* *Licania octandra*										
Rainforest, Au-QLD	*Argyrodendron peralatum* *Syzygium graveolens*	-16.10	145.44	1000	25 – 40	24.3 – 27.5	Natural environmental conditions	April 2011 July 2011	mature	ACi-T	Kelly (2014)
Savanna Eucalypt, AU-NT	*Eucalyptus tetrodonta*	-14.16	131.39	2000	25 – 40	27.1	Natural environmental conditions	September 2008	mature	ACi-T	Cernusak *et al.* (2011)
Norway Spruce, Sweden	*Picea abies*	58.38	12.15	1047	13 – 33	9.3	Natural environmental conditions	June, September 2009 June 2010	mature	ACi-T	Tarvainen *et al.* (2013)
Scots Pine, Sweden	*Pinus sylvestris*	64.16	19.75	1500	15 – 35	15.4	Natural environmental conditions	August 2013	mature	ACi-T	Tarvainen *et al.* (2017)
Subalpine Eucalypt, AU-NSW	*Eucalyptus delegatensis*	-35.66	148.15	1500	12 – 32	11.9	Natural environmental conditions	November 2001 February 2002 May 2002	mature	ACi-T An-T	Medlyn *et al.* (2007)
Scots Pine, Finland	*Pinus sylvestris*	62.78	30.96	1200	5 – 32	14.0	Natural environmental conditions	July 1998	mature	ACi-T	Wang *et al.* (1996)
Eucalyptus tereticornis provs AU-NSW	*Eucalyptus tereticornis* prov. temperate prov. sub-tropical prov. tropical	 -35.39 -26.57 -15.5	 150.07 152.05 145.14	1500	18 – 42	18 – 35.5	Six growth temperature treatments 1. 18°C 2. 21.5°C 3. 25°C 4. 28.5°C 5. 32°C 6. 35.5°C [CO_2] = 400 ppm	February 2016	seedlings	ACi-T	Javier Cano and John E. Drake, Unpublished data
Pinus sylvestris provs, USA-WI	*Pinus sylvestris* prov Haguenau prov Suprasl prov Spala prov Sumpberget prov Ostrovskij prov Prusacka Rijeka	 48.81 53.2 51.61 60.18 57.83 44.08	 7.78 23.36 20.2 15.86 28.15 17.35	1500	15 – 37				seedlings	An-T	Mark G. Tjoelker, Unpublished data. see also Oleksyn, Tjoelker and Reich (1998)
Corymbia calophylla provs, AU-NSW	*Corymbia calophylla* prov Cape Richie prov Boorara prov Mogumber prov Gingin	 -34.6 -34.73 -31.1 -31.34	 118.74 116.21 116.05 115.89	1800	20 – 40	26 .0	Two growth temperature treatments 1. 26°C 2. 32°C	July 2014	seedlings	ACi-T	Aspinwall *et al.* (2017)
Ghannoum Eucalypt spp, AU-NSW	*Eucalyptus saligna,* *Eucalyptus sideroxylon*	-30.57 -32.99	152.15 147.89	1500	15 – 43	22.0	Two growth temperature treatments Ambient - 26°C Elevated - 30°C		seedlings	An-T	Ghannoum *et al.* (2010)

							Three [CO2] treatments Sub-ambient – 280 ppm Ambient – 400 ppm Elevated – 640 ppm				
Dreyer DBF spp, France	*Acer pseudoplatanus* *Betula pendula* *Fagus sylvatica* *Fraxinus excelsior* *Juglans regia* *Quercus petraea* *Quercus robur*	46.37 52.5 50.24 50.2 47.02 48.55 48.55	5.96 7.23 5.05 3.72 6.74 0.08 0.08	1500	10 – 40	17.3	Natural environmental conditions under 45% transmitted global irradiance	July 1994 July 1995	seedlings	ACi-T	Dreyer *et al.* (2001)
Eucalyptus saligna, AU-NSW	*Eucalyptus saligna*	-30.43	152.04	1800	18 – 36	17.7 – 22.6	Two [CO2] treatments Track ambient Elevated – ambient +240 ppm Two watering treatments Wet – well watered Dry -	January 2009 November 2008	saplings	ACi-T	Yan Shih Lin, Unpublished data
Eucalyptus globulus, AU-NSW	*Eucalyptus globulus*	-38.8	143.59	1800	17 – 41	19.7 – 24.9	Two temperature treatments Track ambient Elevated – ambient +3.5°C Two [CO2] treatments Track ambient Elevated – ambient +240 ppm	December 2010 February 2011 August, September 2011	saplings	ACi-T	Crous *et al.* (2013)
Eucalyptus tereticornis, AU-NSW	*Eucalyptus tereticornis*	-33.62	150.74	1800	20 – 42	14.4 – 22.6	Two temperature treatments Track ambient Elevated – ambient +3.5°C	September 2013 January 2014 April 2014 May 2014	saplings	ACi-T	Kristine Crous, Unpublished data
Eucalyptus parramattensis, AU-NSW	*Eucalyptus parramattensis*	-33.62	150.74	1800	17 – 42	15.1 – 18.0	Two temperature treatments Track ambient Elevated – ambient +3.5°C	July 2016 October 2016	saplings	ACi-T	Dushan Kumarathunge, Unpublished data
Eucalyptus globulus, AU-TAS	*Eucalyptus globulus*	-42.81	146.61	1500	10 – 35	10.3 – 14.8	Natural environmental conditions	October 1993 November 1993 February 1994 April 1994 December 1994	saplings	An-T	Battaglia *et al.* (1996)
Black Spruce (Canada)	*Picea mariana*	49.11	-74.61	NA	10 - 40	19 - 27	Two temperature treatments Ambient Elevated –	2005	seedlings	ACi-T	Way & Sage (2008)
Silver Birch	*Betula pendula*	52.5	7.23	1200	5 - 32	unknown	Natural environmental conditions	July 1998	unknown	ACi-T	Wang K-Y, Unpublished data
Monterey pine	*Pinus radiata*	-42.52	172.45	1000	8 – 30		Natural environmental conditions		seedlings	ACi-T	Walcroft *et al.*, (1997)
Smith C3 spp, IN, USA	*Acer rubrum* *Betula alleghaniensis* *Betula papyrifera* *Cedrela odorata* *Cucumis sativa* *Elymus Canadensis* *Glycine max*	Exact seed source locations were unknown.		1200	14 – 50	15 – 35	Five growth temperature treatments (15, 20, 25, 30 and 35°C) [CO2] = 400 ppm		seedlings	ACi-T	Smith and Dukes (2017)

Do not distribute

	Oryza sativa *Pinus nigra* *Pinus pinaster* *Pinus pinea* *Pinus sylvestris* *Poa pratensis* *Tamarindus indica* *Triticum aestivum* *Ulmus americana*									

References

Aspinwall MJ, Vårhammar A, Blackman CJ *et al.* (2017) Adaptation and acclimation both influence photosynthetic and respiratory temperature responses in Corymbia calophylla. Tree Physiology, **37**, 1095-1112.

Battaglia M, Beadle C, Loughhead S (1996) Photosynthetic temperature responses of Eucalyptus globulus and Eucalyptus nitens. Tree Physiology, **16**, 81-89.

Cernusak LA, Hutley LB, Beringer J, Holtum JaM, Turner BL (2011) Photosynthetic physiology of eucalypts along a sub-continental rainfall gradient in northern Australia. Agricultural and Forest Meteorology, **151**, 1462-1470.

Crous KY, Quentin AG, Lin YS, Medlyn BE, Williams DG, Barton CV, Ellsworth DS (2013) Photosynthesis of temperate Eucalyptus globulus trees outside their native range has limited adjustment to elevated CO2 and climate warming. Glob Chang Biol, **19**, 3790-3807.

Dillaway DN, Kruger EL (2010) Thermal acclimation of photosynthesis: a comparison of boreal and temperate tree species along a latitudinal transect. Plant, Cell & Environment, **33**, 888-899.

Drake JE, Vårhammar A, Kumarathunge D *et al.* (2017) A common thermal niche among geographically diverse populations of the widely distributed tree species Eucalyptus tereticornis: No evidence for adaptation to climate-of-origin. Global Change Biology, **23**, 5069-5082.

Dreyer E, Le Roux X, Montpied P, Daudet FA, Masson F (2001) Temperature response of leaf photosynthetic capacity in seedlings from seven temperate tree species. Tree Physiology, **21**, 223-232.

Fürstenau Togashi H, Prentice IC, Atkin OK, Macfarlane C, Prober SM, Bloomfield KJ, Evans BJ (2017) Thermal acclimation of leaf photosynthetic traits in an evergreen woodland, consistent with the co-ordination hypothesis. Biogeosciences Discuss., **2017**, 1-23.

Ghannoum O, Phillips NG, Sears MA, Logan BA, Lewis JD, Conroy JP, Tissue DT (2010) Photosynthetic responses of two eucalypts to industrial-age changes in atmospheric [CO2] and temperature. Plant, Cell & Environment, **33**, 1671-1681.

Han Q, Araki M, Chiba Y (2006) Acclimation to irradiance of leaf photosynthesis and associated nitrogen reallocation in photosynthetic apparatus in the year following thinning of a young stand of Chamaecyparis obtusa. Photosynthetica, **44**, 523-529.

Han Q, Kawasaki T, Nakano T, Chiba Y (2004) Spatial and seasonal variability of temperature responses of biochemical photosynthesis parameters and leaf nitrogen content within a Pinus densiflora crown. Tree Physiology, **24**, 737-744.

Hikosaka K, Nabeshima E, Hiura T (2007) Seasonal changes in the temperature response of photosynthesis in canopy leaves of Quercus crispula in a cool-temperate forest. Tree Physiology, **27**, 1035-1041.

Jensen AM, Warren JM, Hanson PJ, Childs J, Wullschleger SD (2015) Needle age and season influence photosynthetic temperature response and total annual carbon uptake in mature Picea mariana trees. Annals of Botany, **116**, 821-832.

Kelly JW. (2013). Productivity and water use of Australian tree species under climate change, PhD thesis, Sydney, Australia

Lin Y-S, Medlyn BE, De Kauwe MG, Ellsworth DS (2013) Biochemical photosynthetic responses to temperature: how do interspecific differences compare with seasonal shifts? Tree Physiology, **33**, 793-806.

Medlyn BE, Loustau D, Delzon S (2002) Temperature response of parameters of a biochemically based model of photosynthesis. I. Seasonal changes in mature maritime pine (Pinus pinaster Ait.). Plant, Cell & Environment, **25**, 1155-1165.

Medlyn BE, Pepper DA, O'grady AP, Keith H (2007) Linking leaf and tree water use with an individual-tree model. Tree Physiology, **27**, 1687-1699.

Oleksyn, J., Tjoelker, M.G. Reich, P.B. (1998). Adaptation to changing environment in Scots pine populations across a latitudinal gradient. Silva Fennica 32(2): 129–140.

Onoda Y, Hikosaka K, Hirose T (2005) The balance between RuBP carboxylation and RuBP regeneration: a mechanism underlying the interspecific variation in acclimation of photosynthesis to seasonal change in temperature. Functional Plant Biology, **32**, 903-910.

Rogers A, Serbin SP, Ely KS, Sloan VL, Wullschleger SD (2017) Terrestrial biosphere models underestimate photosynthetic capacity and CO2 assimilation in the Arctic. New Phytologist, **216**, 1090-1103.

Slot M, Winter K (2017) In situ temperature response of photosynthesis of 42 tree and liana species in the canopy of two Panamanian lowland tropical forests with contrasting rainfall regimes. New Phytologist, **214**, 1103-1117.

Smith NG, Dukes JS (2017) Short-term acclimation to warmer temperatures accelerates leaf carbon exchange processes across plant types. Global Change Biology, **23**, 4840-4853.

Tarvainen L, Lutz M, Räntfors M, Näsholm T, Wallin G Temperature responses of photosynthetic capacity parameters were not affected by foliar nitrogen content in mature Pinus sylvestris. Physiologia Plantarum, n/a-n/a.

Tarvainen L, Wallin G, Räntfors M, Uddling J (2013) Weak vertical canopy gradients of photosynthetic capacities and stomatal responses in a fertile Norway spruce stand. Oecologia, **173**, 1179-1189.

Tribuzy ES. (2005). Variações da temperatura foliar do dossel e o seu efeito na taxa assimilatória de CO2 na Amazônia Central, PhD thesis, INPA, Manaus, Brazil

Vårhammar A, Wallin G, Mclean CM *et al.* (2015) Photosynthetic temperature responses of tree species in Rwanda: evidence of pronounced negative effects of high temperature in montane rainforest climax species. New Phytologist, **206**, 1000-1012.

Wang K-Y, Kellomäki S, Laitinen K (1996) Acclimation of photosynthetic parameters in Scots pine after three years exposure to elevated temperature and CO2. Agricultural and Forest Meteorology, **82**, 195-217.

Way DA, Sage RF (2008) Thermal acclimation of photosynthesis in black spruce [Picea mariana (Mill.) B.S.P.]. Plant, Cell & Environment, **31**, 1250-1262.